

## Angular Distributions of $\alpha$ Particles from the $\text{Na}^{23}(p,\alpha)\text{Ne}^{20}$ Reaction

P. H. STELSON

*Oak Ridge National Laboratory, Oak Ridge, Tennessee*

(Received August 9, 1954)

The angular distribution of  $\alpha$  particles produced by the  $\text{Na}^{23}(p,\alpha)\text{Ne}^{20}$  reaction and leading to the ground state of the residual  $\text{Ne}^{20}$  nucleus has been measured at six resonances occurring in the region  $E_p = 1$  to 2 Mev. The measured distributions are compared to the calculated angular distributions. In many cases the calculated angular distribution for a given type of compound state is not unique in that an unknown mixture of channel spins enters as well as possible admixtures of higher  $l$  values. The best assignments for the resonances at 1.137, 1.012, and 1.166 Mev are respectively  $0^+$ ,  $3^-$ , and  $2^+$ . A large anisotropy is observed for the resonance at 1.288 Mev which is not predicted by any simple assignment. It can, however, be fitted by a  $1^-$  assignment in which there is a rather large admixture of  $f$ -wave to the  $p$ -wave protons. The resonance at 1.804 Mev is found to be complex.

### I. INTRODUCTION

A PREVIOUS paper<sup>1</sup> (referred to as S.P. hereafter) described the study of the resonant states of  $\text{Mg}^{24}$  from measurements of the yield of  $\gamma$  rays and  $\alpha$  particles when sodium is bombarded by protons. This paper reports on a continuation of this study in which angular distributions of  $\alpha$  particles were measured at several resonances.

Since an angular distribution is governed by the combining of angular momentum vectors during the course of the reaction, one hopes to work back from the measured distribution to the discovery of the particular combination of vectors responsible for the distribution. In this way the total angular momentum and parity of the compound state can be assigned and, in addition, information is obtained on the mixing of channel spins and percentage admixture of higher orbital angular momenta.

In practice, the relatively large number of theoretically possible angular distributions and the limited accuracy of the experimental results make unique assignments difficult. For this reason it was thought that the angular distributions of the  $\alpha$  particles produced by the  $\text{Na}^{23}(p,\alpha)\text{Ne}^{20}$  reaction and leading to the ground state of the residual  $\text{Ne}^{20}$  nucleus ( $\alpha_0$  channel) would give the most clear-cut information. It was pointed out in S.P. that to decay by this channel the compound states must be of the type  $0^+$ ,  $1^-$ ,  $2^+$ ,  $3^-$ , etc., and this restriction cuts down the number of possible distributions to be considered by a factor of two. Furthermore, for a given type of compound state one must consider, in general, an unknown mixture of channel spins and possible admixture of higher  $l$  values in both the entrance and exit channels, while for this case only the channel-spin of zero and one  $l$  value need be considered for the exit channel.

### II. EXPERIMENTAL METHOD

Figure 1 is a schematic diagram of the apparatus used to measure the angular distributions. The proton beam

from the electrostatic generator enters from the left. The beam is trimmed by two pairs of adjustable slits at right angles to each other. A diaphragm shields the reaction chamber by intercepting protons scattered by the slits. Two sylphon bellows allow movement of the chamber for alignment purposes. Alignment is facilitated by the two glass sections containing movable quartz viewers on which cross hairs are marked. The beam current is measured by catching the protons in the insulated, retractable cup which is biased to eliminate electron currents.

The type of counter used to detect the  $\alpha$  particles is similar to that described in S.P., viz., a cylindrical, gas-filled proportional counter fitted with a thin nickel window. The discussion of the method by which it singles out the ground state  $\alpha$  particles is given in S.P. Detail A in Fig. 1 is a schematic diagram of the counter. Differential bias curves at several angles with respect to the forward direction and at two proton energies are shown in Fig. 2. It is seen that this relatively simple method of detecting the ground state  $\alpha$  particles is not reliable at the forward angles due to the large pile-up of elastically scattered protons. The effect becomes more serious for low proton energies. For this reason the distributions could not be extended to the forward angles.

The counter window (diameter of 0.4 cm) was placed 7 cm from the target. The angular spread is  $3^\circ$  or the maximum  $\Delta x$ , where  $x = \cos\theta_{\text{c.m.}}$ , is 0.05 at  $90^\circ$ . With this angular resolution the attenuation coefficients for  $P_2(x)$  and  $P_4(x)$  differ from unity by a negligible amount (see Rose<sup>2</sup>). The angular spread caused by the finite size of the source is, on the average, about one-half as large as that due to the counter window.

The alignment of the counter with respect to the proton beam was carried out in the following manner. The center of the circle on which the counter swings was located by measuring the variation with angle position of the counting rate of  $\alpha$  particles from a  $\text{U}^{233}$  source placed on the target support. The chamber was then moved to make the proton beam hit this point. A

<sup>1</sup> P. H. Stelson and W. M. Preston, Phys. Rev. **95**, 974 (1954).

<sup>2</sup> M. E. Rose, Phys. Rev. **91**, 610 (1953).

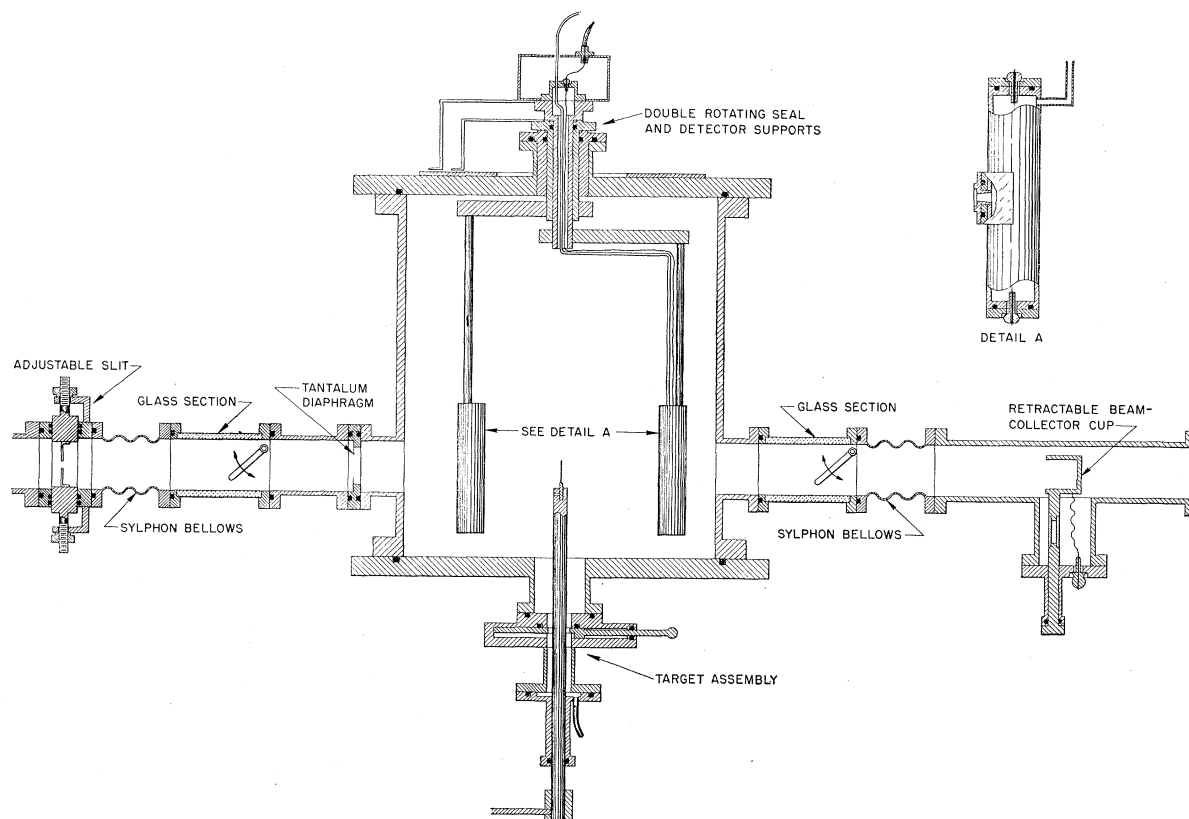


FIG. 1. Reaction chamber.

check on the alignment was made by counting protons elastically scattered from the target on both sides of the forward direction. It is judged that for the  $(p, \alpha)$  angular distributions measurements the variation of the solid angle with angular position is not more than 3 percent.

Since we wished to investigate several fairly sharp resonances, it was thought that normalizing with respect to beam current would not be reliable because of the difficulty in maintaining a constant proton energy and constant target condition over long bombardment periods. Therefore, counts were collected in a second, stationary  $\alpha$  particle counter and used to normalize the data. Changes in target condition and/or drifts in the proton energy were noted from the ratio of counts in the stationary counter to beam current collected.

Targets were prepared by vacuum evaporation of sodium iodide onto thin  $[25\text{-mg/cm}^2]$  Formvar backings. By means of the valve arrangement shown in Fig. 1, a target could be admitted without disturbing the vacuum in the chamber. The proton beam at the target was a 3 mm square. Currents were limited to approximately  $\frac{1}{10} \mu\text{amp}$  to keep the targets from burning up.

The angle  $\phi$  between the plane of the target and the plane perpendicular to the beam is variable. For a fixed angle  $\phi$ , the area of the source changes for different angular positions of the detector. A check on whether

this might cause errors was made by keeping the counter in a fixed position and measuring the counting rate caused by elastically scattered protons for different values of  $\phi$ . It was determined that for the angles of  $\phi$  used in the angular distribution measurements the variation is less than one percent.

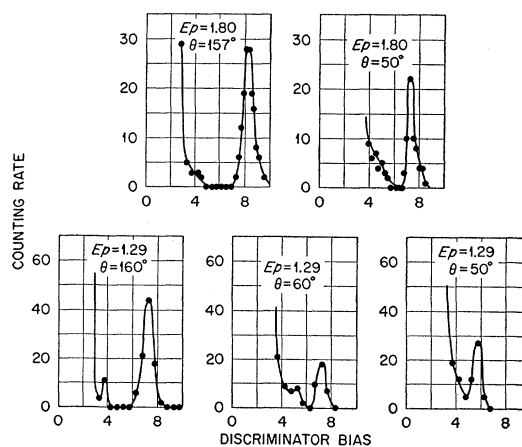


FIG. 2. Differential bias curves at several angles with respect to the forward direction and at two proton energies. The peak observed at high bias values is due to particles in the  $\alpha_0$  channel. The large rise at low bias is due to scattered protons. The weak intermediate peak observable in two of the curves is due to particles in the  $\alpha_1$  channel.

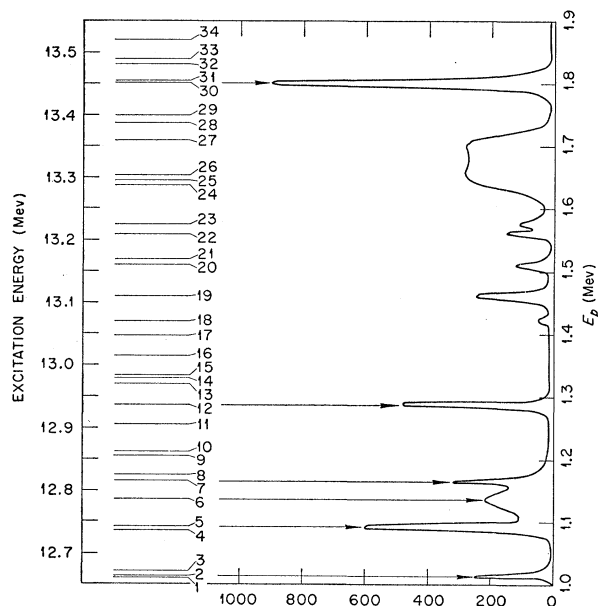


FIG. 3. Yield of  $\alpha$  particles produced by the  $\text{Na}^{23}(p,\alpha)\text{Ne}^{20}$  reaction and leading to ground state of  $\text{Ne}^{20}$  (taken from S.P.) and the positions of the virtual states of  $\text{Mg}^{24}$  for the region  $E_p=1.0$  to 1.9 Mev.

### III. RESULTS

#### Resonance No. 12

A yield curve of the  $\alpha$  particles in the  $\alpha_0$  channel and an energy level diagram of the virtual states of  $\text{Mg}^{24}$  occurring in the region  $E_p=1.0$  to 1.9 Mev is given in Fig. 3.<sup>3</sup> Resonance No. 12 ( $E_p=1.288$  Mev) was thought to be especially suitable for study because it is well removed from neighboring resonances and has a

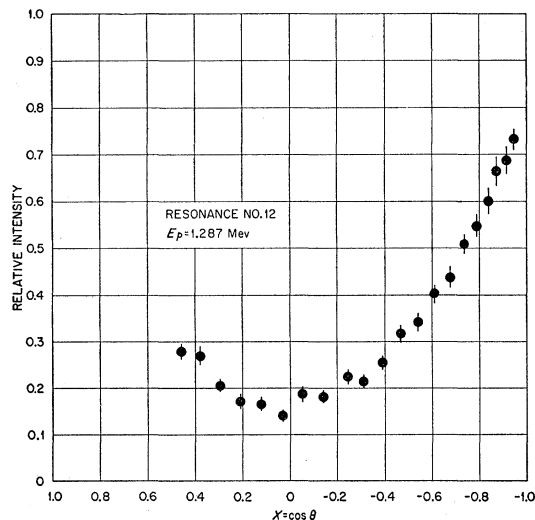


FIG. 4. Angular distribution of the ground state  $\alpha$  particles at Resonance No. 12 ( $E_p=1.288$  Mev). Data have been transformed to center-of-mass system.

<sup>3</sup> The numbers assigned to the resonances are those given in S.P.

large cross section for decay by the  $\alpha_0$  channel. A yield curve of the  $\alpha$  particles showed that the thickness of the target used for measurements was 10 kev. The yield curve also indicated a small yield at proton energies well removed from the resonance. This flat continuum, which was found to be isotropic, may be the tail of the broad Resonance No. 6 which is also isotropic.

The possibility that the angular distribution is being disturbed by interference from neighboring resonances must be borne in mind. A single, well-isolated resonance must exhibit symmetry about  $x=0$ . Although the yield at the more forward angles could not be measured, the existing data suggest symmetry about  $x=0$ . Furthermore, the angular distribution of an isolated resonance should be independent of the point on the resonance at which it is measured, while an interference should cause the distribution to change as the resonance is traversed. To check this point, the ratios of the yield at  $x=-0.05$  and  $-0.94$  were measured half-way up the leading edge, on the maximum and half-way down the back edge. No change in the ratios of the yields was observed. This is taken as evidence that the small continuum is not perturbing the angular distribution. The continuum has been subtracted in analyzing the data. At  $x=0$ , where the differential cross section of the resonance has its lowest value, the continuum amounted to 20 percent. The angular distribution at the peak of the resonance is shown in Fig. 4.

The data from several runs of the angular distribution on the maximum of the resonance were fitted by a least-squares analysis to the expression

$$B_0P_0(x) + B_2P_2(x) + B_4P_4(x), \quad (1)$$

where the  $P_i(x)$  are Legendre polynomials. The coefficient  $B_4$  was found to be zero to within the expected errors. The ratio  $B_2/B_0$  is listed in Table I. The assigned error is based on the statistical accuracy of the points and an estimate of the errors discussed in Part II.

#### Resonance No. 2

Resonance No. 2 ( $E_p=1.012$  Mev) has a close neighbor on each side. However, the yield curve indicates that neither of these neighboring resonances decays by the  $\alpha_0$  channel and, hence, is not expected to distort the angular distribution of the ground state  $\alpha$  particles. The angular distribution at the maximum of the resonance is shown in Fig. 5. The yield curve showed no measurable continuum in the region of this resonance. The ratios of the yields at  $x=-0.05$  and  $-0.94$  taken half-way up the leading edge, at the maximum, and half-way down the back edge showed no significant variation. The data were fitted to expression (1). The coefficient  $B_4$  was not significantly different from zero. The ratio  $B_2/B_0$  and its error are listed in Table I.

## Resonances No. 30 and No. 31

Although the poorer resolution of the  $\alpha$ -particle yield curve shows a strong, isolated resonance at 1.80 Mev, the high-resolution  $\gamma$ -ray yield curves reveal two resonances separated by 3 kev. Yet because of the selection rules operative in the  $\alpha_0$  channel there is a good chance that just one of the resonances is decaying by the  $\alpha_0$  channel. The angular distribution of the maximum of the peak is found to be symmetric about  $x=0$ . However, the ratios of the yields at  $x=-0.05$  and  $-0.94$ , which are listed in Table I, varied well outside of the statistical errors at different points on the resonance. This is taken as evidence that both resonances are decaying by the  $\alpha_0$  channel. No further study was made of the resonance because of this complication.

## Resonance No. 6

Resonance No. 6 ( $E_p=1.137$  Mev) is a broad, fairly strong resonance which appeared with measurable intensity only in the yield of the ground state  $\alpha$  particles.

TABLE I. Experimental values of  $B_2/B_0$ .  $E_p$  is given in Mev. The change in the ratio of the yield at  $x=-0.94$  to  $-0.05$  is listed for the resonance at 1.804 Mev.

Resonance number	$E_p$ (Mev)	$B_2/B_0$
2	1.012	$0.86 \pm 0.09$
5	1.093	$0.15 \pm 0.05$
6	1.137	$0.05 \pm 0.05$
7	1.166	$0.03 \pm 0.05$
12	1.288	$1.16 \pm 0.09$
(30+31)?	1.804	
Half-way up leading edge:		$I(x=-0.94)/I(x=-0.05) = 1.32 \pm 0.06$
At the peak:		$I(x=-0.94)/I(x=-0.05) = 1.72 \pm 0.05$
Half-way down the back edge:		$I(x=-0.94)/I(x=-0.05) = 1.78 \pm 0.11$

Although Resonances No. 5 and No. 7 are situated on the wings of No. 6, these are fairly sharp resonances and should not influence the angular distribution at the maximum. The distribution at the maximum is shown in Fig. 6. The least-squares fit to expression (1) gives a  $B_4$  equal to zero.  $B_2/B_0$  and its assigned error are listed in Table I.

## Resonances No. 5 and No. 7

As previously mentioned, Resonances No. 5 ( $E_p=1.093$  Mev) and No. 7 ( $E_p=1.166$  Mev) are situated on the wings of the broad Resonance No. 6. A moderately thin target of 6-kev thickness was used to reduce the intensity of No. 6 at the positions of No. 5 and No. 7. With this target the contribution of No. 6 to the intensity at the maxima of No. 5 and No. 7 is estimated as roughly 20 percent. The angular distribution at the maximum of No. 7 is found to be isotropic;  $B_2/B_0$  and its error are listed in Table I. No. 5 exhibits

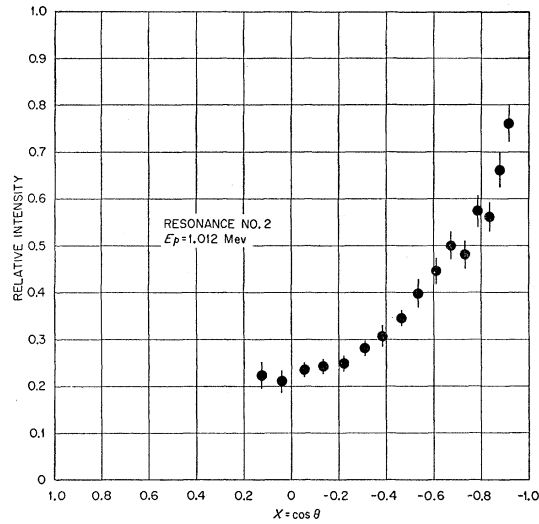


FIG. 5. Angular distribution of the ground state  $\alpha$  particles at Resonance No. 2 ( $E_p=1.012$  Mev). Data have been transformed to center-of-mass system.

a definite, but weak anisotropy;  $B_2/B_0$  and its error are listed in Table I. A check on the invariance of the angular distribution at different points on the resonance was not carried out for these resonances.

## IV. DISCUSSION

## 1. Theory

We use the theory and terminology of angular distributions given by Blatt and Biedenharn<sup>4</sup> to interpret the measured distributions. Compound states of the type  $0^+$ ,  $1^-$ ,  $2^+$ ,  $3^-$ , and  $4^+$  are considered. It is thought

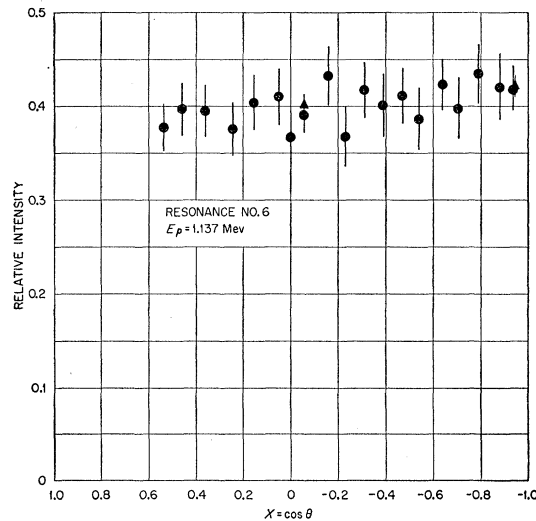


FIG. 6. Angular distribution of the ground state  $\alpha$  particles at Resonance No. 6 ( $E_p=1.137$  Mev). Data have been transformed to center-of-mass system.

<sup>4</sup> J. M. Blatt and L. C. Biedenharn, Revs. Modern Phys. 24, 258 (1952).

quite unlikely that we are dealing with any  $5^-$  (or larger  $J$  value) states since decay through the  $\alpha_0$  channel would require 5 or more units of orbital angular momentum for the  $\alpha$  particles. The resulting small penetrability would strongly suppress the cross section in the  $\alpha_0$  channel.

The target nucleus,  $\text{Na}^{23}$ , with spin  $\frac{3}{2}$  combines with the proton with spin  $\frac{1}{2}$  to give rise to the two values 1 or 2 for the channel spin (denoted by  $s$ ) in the entrance channel. The channel spin, in turn, combines with the orbital angular momentum of the proton [denoted by  $l(p)$ ] to form the compound state (denoted by  $J^{\text{parity}}$ ). The different vector combinations by which each of the above-mentioned compound states can be formed are listed in Table II. Also listed are the coefficients

TABLE II. The different vector combinations by which each of the compound states  $0^+$ ,  $1^-$ ,  $2^+$ ,  $3^-$ , and  $4^+$  of  $\text{Mg}^{24}$  can be formed by protons on sodium and subsequently decay by  $\alpha$ -particle emission to the ground state of  $\text{Ne}^{20}$  are listed. The entrance channel spin is  $s$  while  $l_p$  is the proton orbital angular momentum,  $l_\alpha$  the  $\alpha$ -particle orbital angular momentum, and  $s'$  the exit channel spin. Also listed are the coefficients  $B_2/B_0$ ,  $B_4/B_0$ , etc., which give the angular distribution to be expected for each of these vector combinations.

$s$	$l_p$	Compound state	$l_\alpha$	$s'$	$B_2/B_0$	$B_4/B_0$	$B_6/B_0$	$B_8/B_0$
2	2	$0^+$	0	0	0	0	0	0
1	1	$1^-$	1	0	-1.00	0	0	0
2	1		1	0	+0.20	0	0	0
2	3		1	0	+0.80	0	0	0
2	0	$2^+$	2	0	0	0	0	0
2	2		2	0	-0.51	+0.73	0	0
1	2		2	0	+0.71	-1.71	0	0
2	4		2	0	+1.02	+0.55	0	0
2	1	$3^-$	3	0	+0.80	0	0	0
2	3		3	0	+0.42	-0.82	+1.26	0
1	3		3	0	+1.00	+0.27	-2.27	0
2	2	$4^+$	4	0	+1.02	+0.55	0	0
2	4		4	0	+1.10	+0.73	-0.09	-2.74
1	4		4	0	+0.74	-0.72	-0.93	+1.75

coefficients  $B_2/B_0$ ,  $B_4/B_0$ , etc., which give the angular distribution to be expected for each of these vector combinations.

Now, one expects that a given type of compound state is excited to some extent by each of the possible vector combinations. The mixing of combinations must be considered in order to compare with experiment. We assign to each vector combination the parameter  $g_{s, l(p)}$  where  $g_{s, l(p)} = \pm (\Gamma_{s, l(p)})^{\frac{1}{2}}$ ,  $\Gamma_{s, l(p)}$  being the partial width for the particular combination  $s, l(p)$ . If two different orbital angular momenta,  $l(p)$  and  $l(p)+2$ , can combine with one channel spin to form a given compound state, an interference of the  $l(p)$  and  $l(p)+2$  waves exists. Formula (5.9) of reference 3 is used to calculate the variation of the coefficients  $B_2/B_0$ ,  $B_4/B_0$ ,

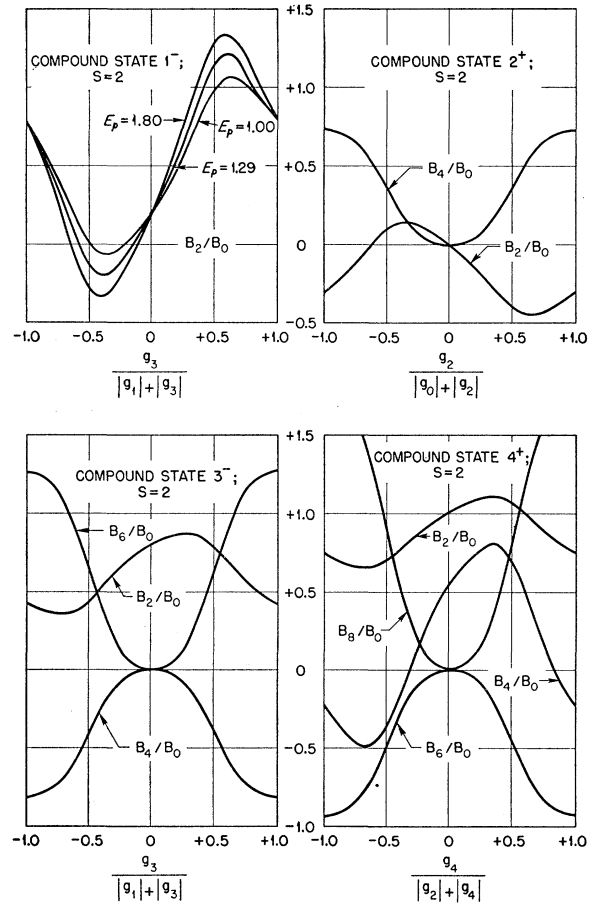


FIG. 7. Calculated curves showing the coherent interference resulting from mixtures of  $l_p$  values in a given channel spin  $s$ . The variation in  $B_2/B_0$ ,  $B_4/B_0$ , etc., is shown as  $\delta$  (defined in the text) varies from  $-1$  to  $0$  to  $+1$ .

etc., for different values of the ratio

$$\delta = g_{s, l(p)+2} / |g_{s, l(p)}| + |g_{s, l(p)+2}|,$$

ranging from 1 to 0 to  $-1$ . The formula contains the phase difference  $\xi_{l(p)+2} - \xi_{l(p)}$ . For a single, isolated resonance the phase difference is given by

$$\xi_{l(p)+2} - \xi_{l(p)} = \left[ \tan^{-1} \left( \frac{\eta}{l(p)+2} \right) + \tan^{-1} \left( \frac{\eta}{l(p)+1} \right) \right] - \left[ \tan^{-1} \left( \frac{F_{l(p)+2}}{G_{l(p)+2}} \right) - \tan^{-1} \left( \frac{F_{l(p)}}{G_{l(p)}} \right) \right],$$

where  $\eta = Z_1 Z_2 e^2 / \hbar v$  and the Coulomb wave functions  $F$  and  $G$  are evaluated at the nuclear surface. The contribution of the terms involving  $F$  and  $G$  (second bracket) is almost negligible for the present situation so that the phase difference is insensitive to the value taken for the nuclear radius. The phase difference depends on the energy of the incident proton so that

the strength of the interference changes somewhat at different resonances. These interference effects have been worked out for all the cases listed in Table II for  $E_p=1.0$  Mev (Resonance No. 2) except the admixture of  $l(p)=4$  for the  $2^+$  resonance. The interference effect for the  $1^-$  state has also been calculated for  $E_p=1.29$  Mev (Resonance No. 12) and  $E_p=1.80$  Mev (Resonances No. 30 and No. 31) to illustrate the change with proton energy. The calculations are presented in Fig. 7 in the form of curves showing the variation of  $B_2/B_0$ ,  $B_4/B_0$ , etc., as a function of  $\delta$ .

It is seen that the interference may strongly affect the shape of the angular distribution. Perhaps the most striking case is the interference of  $p$ -wave and  $f$ -wave protons for  $s=2$ , compound state  $1^-$ , which is given in the upper left-hand corner of the figure. An  $f$ -wave contribution of one percent to the intensity of the resonance ( $\delta=\pm 0.10$ ) will change the  $B_2/B_0$  ratio from  $+0.20$  to  $+0.05$  or  $+0.35$  depending on the sign of  $\delta$ .

Designating  $T_{l(p)}$  as the penetration factor for protons of orbital angular momentum  $l(p)$  through the Coulomb plus centrifugal barrier and  $\gamma_{l(p)}^2$  as the reduced width for the formation of the compound state by  $l(p)$  protons, we can express  $|\delta|$  as

$$\frac{(\gamma_{l(p)+2}^2/\gamma_{l(p)}^2)^{\frac{1}{2}}(T_{l(p)+2}/T_{l(p)})^{\frac{1}{2}}}{1+(\gamma_{l(p)+2}^2/\gamma_{l(p)}^2)^{\frac{1}{2}}(T_{l(p)+2}/T_{l(p)})^{\frac{1}{2}}}.$$

The quantity  $[T_{l(p)+2}/T_{l(p)}]^{\frac{1}{2}}$  varies with proton energy and with  $l(p)$ . For the resonances and  $l(p)$  values here considered the value is of the order of  $1/10$  to  $1/20$ .

Little is known about the values to expect for the quantity  $[\gamma_{l(p)+2}^2/\gamma_{l(p)}^2]^{\frac{1}{2}}$ . If the compound state were a simple, single particle state in which  $l(p)$  is a good quantum number (quite unlikely at these high excitation energies) one would expect the values zero or infinity depending on whether the compound state is characterized by  $l(p)$  or  $l(p)+2$ . On the other hand, if the compound state is sufficiently complicated one expects a statistical picture to prevail in which case  $[\gamma_{l(p)+2}^2/\gamma_{l(p)}^2]^{\frac{1}{2}}$  is unity.

If  $[\gamma_{l(p)+2}^2/\gamma_{l(p)}^2]^{\frac{1}{2}}$  is unity, the small values of  $1/10$  to  $1/20$  for  $[T_{l(p)+2}/T_{l(p)}]^{\frac{1}{2}}$  limit the possible values of  $\delta$  to a small region of approximately  $\pm 0.10$  about the zero point. If the statistical picture is correct, we should be able to fit the data with the restriction that  $|\delta| \lesssim 0.10$ . However, if larger values of  $\delta$  are required we have a measure of the deviation from the strictly statistical model.

Finally, when both channel spins can contribute to the excitation of a given type of resonance, mixtures of these must also be considered. Since the two channels are incoherent this is considerably easier to work out than mixtures of  $l(p)$  values. Mixtures are obtained by simply adding together different percentages of the angular distribution in each channel. When the minimum value of  $l(p)$  differs by 2 units for the two chan-

nels, the contribution to angular distribution of the channel with the larger value is strongly suppressed since it is governed by the ratio  $T_{l(p)+2}/T_{l(p)}$  which is of the order of  $1/100$  to  $1/400$ .

## 2. Assignments

### Resonance No. 6

The broad Resonance No. 6 has a measured  $B_2/B_0$  value of  $0.05 \pm 0.05$ . This small value, which is consistent with isotropy, can be fitted by three alternative assignments: (1) a  $0^+$  assignment, which is isotropic, (2) a  $2^+$  assignment in which there is a reasonably small admixture of  $d$ -wave to the  $s$ -wave protons, or (3) a  $1^-$  assignment in which there is a fortuitous combination of mixtures to give a distribution close to isotropic. The probability is small that the  $1^-$  assignment is the correct one. While the angular distribution is equally well accounted for by either the  $0^+$  or the  $2^+$  assignment, the fact that this resonance shows a strong preference for decay by the  $\alpha_0$  channel favors the  $0^+$  state. A  $2^+$  state would be expected to show a strong decay by the  $\alpha_1$  and  $p_1$  channels.<sup>5</sup>

### Resonance No. 2

Resonance No. 2, with a measured value of  $0.86 \pm 0.09$  for  $B_2/B_0$  and a  $B_4/B_0$  of zero, agrees well with a  $3^-$  assignment. The value of  $[T_3/T_1]^{\frac{1}{2}}$  is calculated to be  $0.050$ . If  $[\gamma_3^2/\gamma_1^2]^{\frac{1}{2}}$  is taken as unity, we have  $\delta = \pm 0.050$ , both of which give the value of approximately  $0.80$  for  $B_2/B_0$  (see Fig. 7). The reaction goes by the  $s=2$  channel since  $f$ -wave protons are required in the  $s=1$  channel.

Two other assignments of  $4^+$  and  $1^-$  are conceivable but require large values of the order of  $10$  for the quantity  $[\gamma_{l(p)+2}^2/\gamma_{l(p)}^2]^{\frac{1}{2}}$ .

### Resonances No. 5 and No. 7

The fact that these resonances are not well isolated makes assignment somewhat tenuous. No assignment is given to No. 5 which showed a weak anisotropy. Resonance No. 7 is isotropic; hence the possibilities listed under No. 6 should also apply here. Of these, the  $2^+$  state is favored because, in contrast to No. 6, the resonance exhibits a strong decay by the  $\alpha_1$  channel and an observable decay by the  $p_1$  channel.

### Resonance No. 12

Resonance No. 12 has a  $B_2/B_0$  of  $1.16 \pm 0.09$  and no observable  $B_4$  term. This large anisotropy of a pure  $P_2$  type is not given by any assignment in which  $\delta$  is restricted to the small value it would have if  $[\gamma_{l(p)+2}^2/\gamma_{l(p)}^2]^{\frac{1}{2}}=1$ . An assignment of  $1^-$  can be made

<sup>5</sup> The channels  $\alpha_1$  and  $p_1$  are those, respectively, in which the compound state decays to the first excited states of  $\text{Ne}^{20}$  (1.63 Mev) and  $\text{Na}^{23}$  (0.44 Mev).

to give a sufficiently large, positive  $B_2/B_0$  if we simultaneously require that  $\delta \geq +0.45$  and that the reaction goes mostly by the  $s=2$  channel. The large value of  $\delta$  demands the rather high value of 5 or greater for  $[\gamma_3^2/\gamma_1^2]^{\frac{1}{2}}$ . If this assignment is correct, we have an indication that  $[\gamma_{l(p)+2}/\gamma_{l(p)}]^{\frac{1}{2}}$  may undergo large deviations from unity. It would be desirable to measure

angular distributions of other reaction products at this resonance to corroborate or disprove this assignment.

The author wishes to thank Dr. Albert Simon for several discussions of the theory of angular distributions and the members of the High Voltage Group of the Oak Ridge National Laboratory for their interest and cooperation.

## Proton Polarization in $(d,p)$ Reactions\*†

W. B. CHESTON

University of Minnesota, Minneapolis, Minnesota

(Received July 16, 1954)

The polarization of the proton produced in a  $(d,p)$  reaction is calculated under the assumption that "stripping" is the primary mechanism operative. The model adopted for the polarization production consists in a proton-nucleus interaction potential of the spin-orbit type which has been successful in describing polarization effects in neutron scattering. The model is applied to the specific reaction  $C^{12}(d,p)C^{13}$  for  $E_d=3.29$  Mev.

### I. INTRODUCTION

THE apparent usefulness of  $(d,p)$  and  $(d,n)$  reactions as tools in nuclear spectroscopy stems from the now classic paper on these reactions by Butler.<sup>1</sup> The form of the differential cross section for such reactions predicted by the stripping theory is in surprisingly good agreement with the experimental results, especially if deuterons of not too low an energy are used as projectile particles. However, the results of experiments using deuterons of about 3 Mev exhibit features which the stripping theory has difficulty in explaining, even if the modifications<sup>2</sup> of the theory suggested subsequent to Butler's paper are taken into account. Particular reference is made here to the pronounced "resonances" observed in the excitation function and the form of the differential cross sections measured off and on resonance.<sup>3</sup> In brief summary, the resonance behavior of the excitation function is caused by a very pronounced change in magnitude of the forward-angle stripping peak whereas the back-angle yield is relatively constant over the range of energies including the resonances.

It has been suggested<sup>4-6</sup> that the nucleon produced as

a product in the stripping reaction is polarized. The model sketched below for producing such polarization was chosen because of its apparent reasonableness in that such a model correctly describes the elastic scattering of polarized neutrons<sup>7</sup> in the medium-energy range. Since the stripping approximations are used throughout the polarization calculation, the extent of disagreement between the herein predicted polarization and the eventually forthcoming experimental results will indicate the extent to which the stripping assumptions are suspect at the deuteron energies considered below, namely,  $E_d \sim 3$  Mev.

### II. POLARIZATION CALCULATION

In the so-called "Born approximation" discussion<sup>8</sup> of stripping reactions, the final state nucleon is assumed to have no specifically nuclear interaction with the residual nucleus and no polarization of the proton results. In the calculation below, the assumption will be made that the final state nucleon is scattered in a spin-orbit potential superimposed upon the "clouded crystal ball" or complex central potential of Feshbach *et al.*<sup>9</sup> which adequately describes the elastic scattering of low-energy neutrons.<sup>10</sup> Strictly speaking, therefore, the model applies to  $(d,n)$  reactions; it will be applied to  $(d,p)$  reactions as well, with justification supplied by the

\* This work was supported in part by the joint program of the Office of Naval Research and the U. S. Atomic Energy Commission.

† The results of this calculation were first reported at the Minneapolis meeting of the American Physical Society, June, 1954.

<sup>1</sup> S. T. Butler, Proc. Roy. Soc. (London) **A208**, 559 (1951).

<sup>2</sup> See, for example, W. Tobocman and M. H. Kalos, Phys. Rev. **95**, 605(A) (1954).

<sup>3</sup> Van Patter, Simmons, Stratton, and Zipoy, Bull. Am. Phys. Soc. **29**, No. 5, 14 (1954).

<sup>4</sup> H. C. Newns, Proc. Phys. Soc. (London) **A401**, 477 (1953).

<sup>5</sup> J. Horowitz and A. Messiah, Phys. Rev. **92**, 1326 (1953).

<sup>6</sup> N. Francis and K. Watson, Phys. Rev. **93**, 313 (1954). The model used in the present discussion was suggested in this article.

<sup>7</sup> Darden, Fields, and Adair, Phys. Rev. **93**, 931 (1954).

<sup>8</sup> See, for example, P. Daitch and J. French, Phys. Rev. **87**, 900 (1952).

<sup>9</sup> Feshbach, Porter, and Weisskopf, Phys. Rev. **90**, 166 (1953).

<sup>10</sup> Note, however, that the depth of the well suggested by Feshbach *et al.* to explain the scattering data is too small by a factor  $\sim 2$  to harmonize with the data on neutron bound states interpreted on the basis of the shell model. [See A. Bohr and B. Mottelson, Kgl. Danske Videnskab. Selskab, Mat.-fys. Medd. **27**, 159 (1953); R. K. Adair, Phys. Rev. **94**, 737 (1954).]